Figure S1

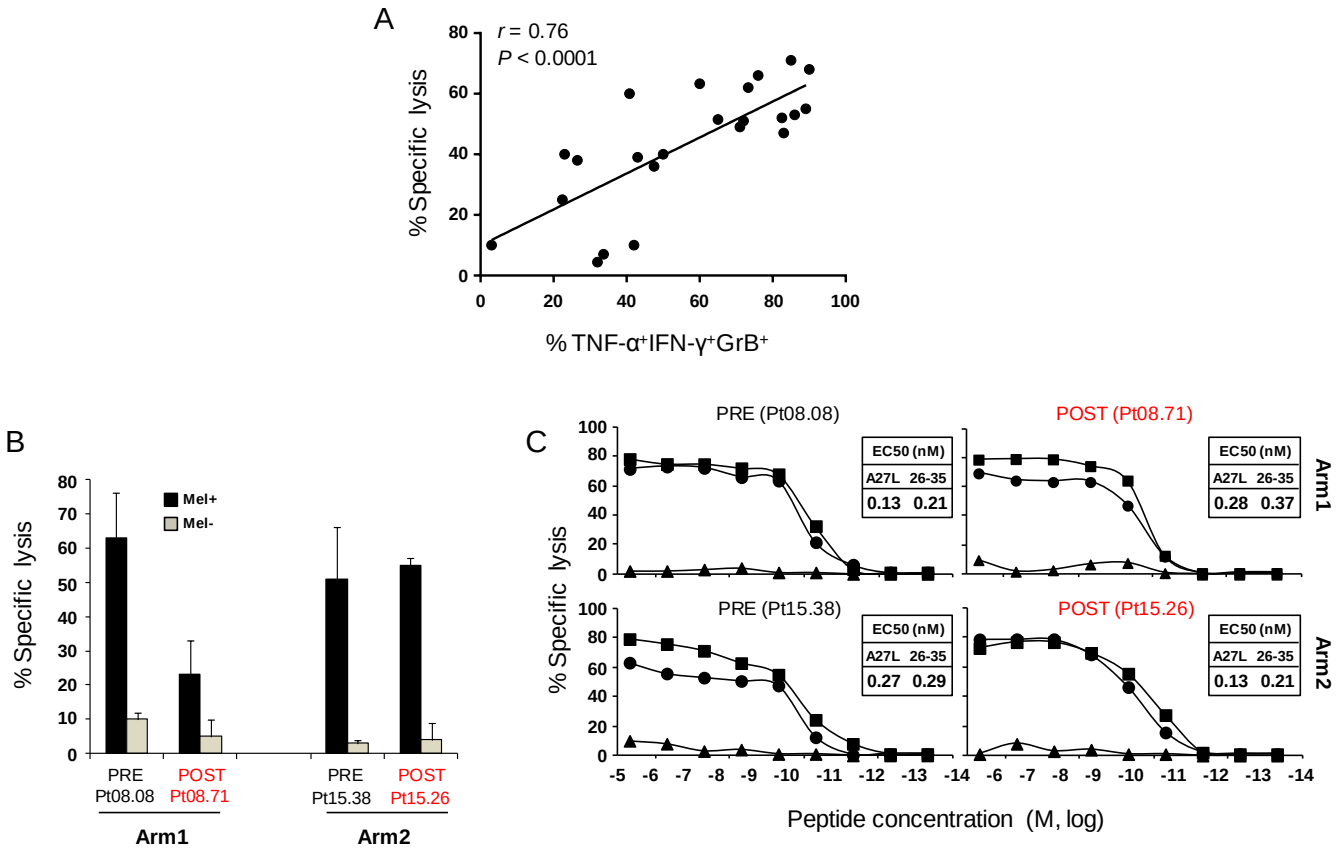

Figure S1. Tumor-specific functional activity of Melan-A specific T-cell clones. (**A**) Scatter plots of tumor lysis %, as measured by 51Cr assay, *versus* the % of TNF-α, IFN-γ, GrB co-production measured by ICS, showing a statistically significant positive correlation. Each point represents the mean percentage out of three independent experiments for each Melan-A+ T-cell clone analyzed. The solid line shows the best line fitted to the data based on a simple regression model. Statistical analysis was performed with both Spearman (shown in figure) and Pearson tests (r = 0.75, $P < 0.0001$). (**B**) Lytic activity of T-cell clones reported in Figure 1A, isolated before (PRE) and at the end (POST) of both therapies.was analyzed by ^{51}Cr assay against A2+/Melan-A+ (Mel+) and A2+/Melan-A- (Mel-) melanoma cell lines, at an E:T ratios of 20:1. Data represent the mean ± SD of three independent experiments. (**C**) Fine antigen specificity analysis, performed on the same T-cell clones, measured by cytotoxicity assay using T2 target cells pulsed with decreasing concentrations of natural Melan-A26-35 (●), analogue Melan-AA27L (■) or irrelevant gp100 (▲) peptides. Inset, avidity of T cells, defined as the concentration of peptide required for half-maximal lysis (EC_{50}), is shown.

Figure S2

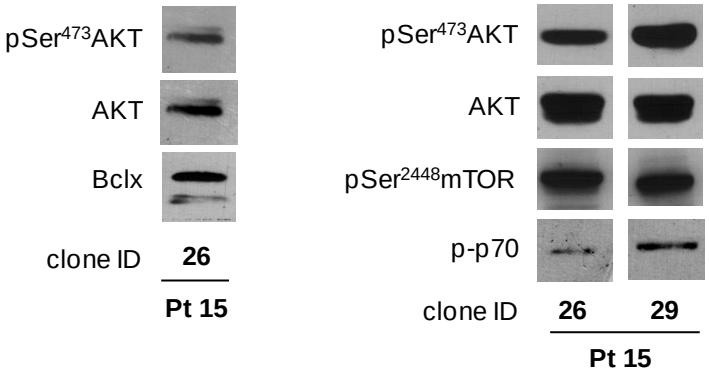

Figure S2. Chemoimmunotherapy mediates the activation of AKT downstream substrate targets. Western Blot analysis of AKT and downstream substrate target activation: pSer473-AKT, Bclx pSer^{2448} (left panel), mTOR and pp70 (right panel), tested on whole cell extracts of 1.5 x10^{6} viable cells of representative Melan-A-specific clones isolated after treatment (POST) from Pt15 of Arm2, 18 h following activation by plated-coated anti-CD3 mAb.

Figure S3

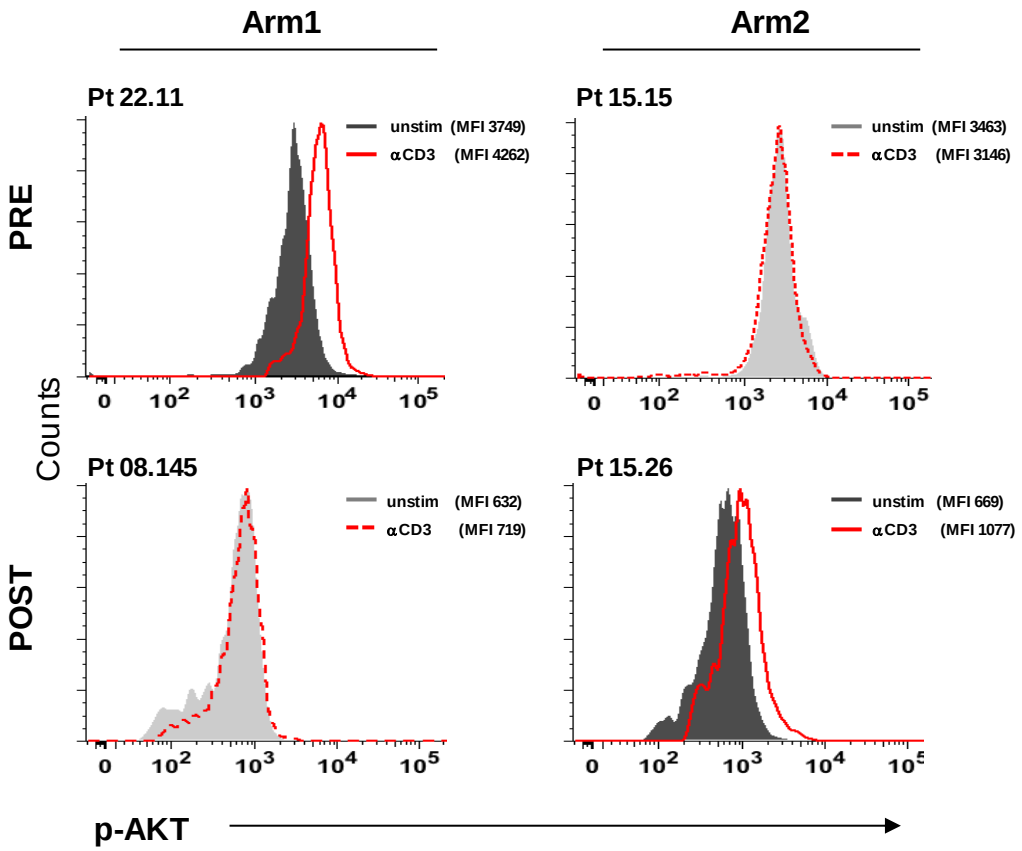

Figure S3. Analysis of pSer473-AKT expression by flow cytometry. Representative histograms of intracellular pSer^{473}AKT flow cytometry in four Melan-A-specific T-cell clones isolated from Arm1 (Pt22.11 and Pt08.145) and Arm2 (Pt 15.15 and Pt 15.26) patients, before (PRE) and after (POST) treatments, unstimulated (unstim) or stimulated (αCD3) for 2 h with anti-CD3 mAb. MFI = mean fluorescence intensity.

Figure S4

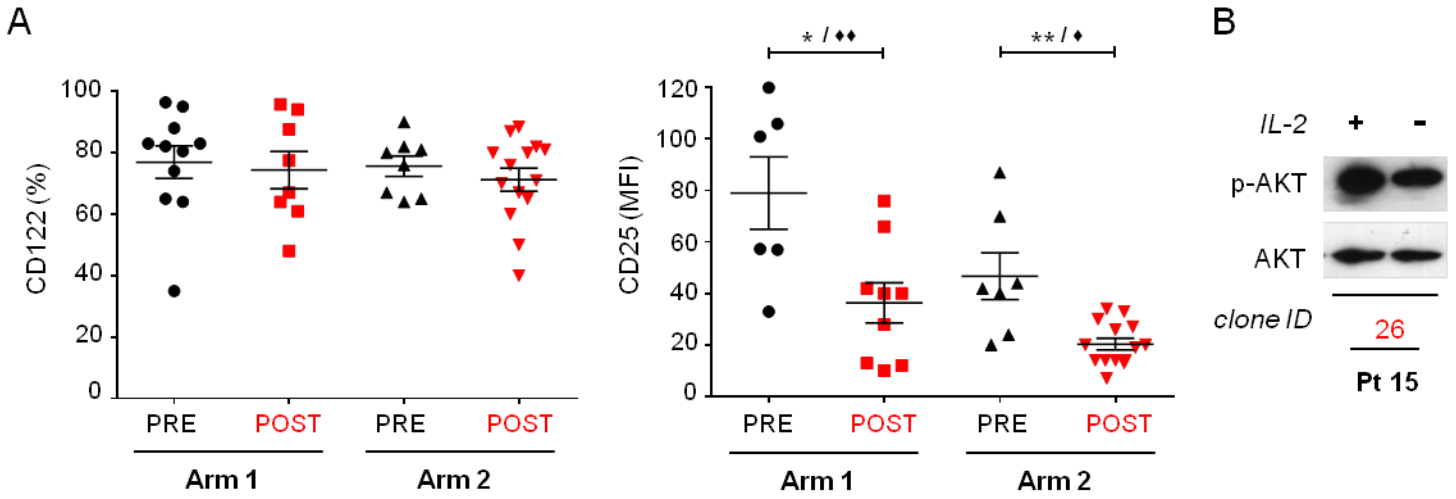

Figure S4. Modulation of IL-2/IL-15R pathway is independent of the different vaccination treatments. (**A**) IL-2/15Rβ and IL-2Rα expression in Melan-A-specific T-cell clones before (PRE) and after (POST) treatments. T-cell clones isolated from Arm1 (n = 6-11 PRE, n = 8-9 POST) and Arm2 (n = 7-8 PRE, n = 13-14 POST) were stained with anti IL-2/15Rβ (CD122, left panel) and IL-2Rα (CD25, right panel) mAbs. Each dot represents the mean value out of three-five independent experiments performed. The mean ± SEM is shown. As evidenced, a similar expression of CD122 was observed in all the clones analyzed, irrespective from treatment. Decreased levels of CD25 were observed in cells isolated after therapy, irrespective from the treatment. $^{*/\blacklozenge}$ $P \leq 0.05$, $^{**/\blacklozenge\blacklozenge}$ $P \leq 0.01$, Mann-Whitney two-sample test and two-tail Student's test, respectively. (**B**) Western Blot analysis of AKT activation (pSer473-AKT), tested on whole cell extracts of 1.5 x10^6 viable cells of a representative Melan-A-specific clone isolated after treatment from Pt15 (Arm2), 18 h following activation by plate-coated anti-CD3 mAb in the presence (+) or in the absence (-) of rIL-2 (25 U/ml). Deprivation of IL-2 from culture medium did not abrogate AKT phosporylation. Data is representative of three independent experiments with similar results.

Figure S5

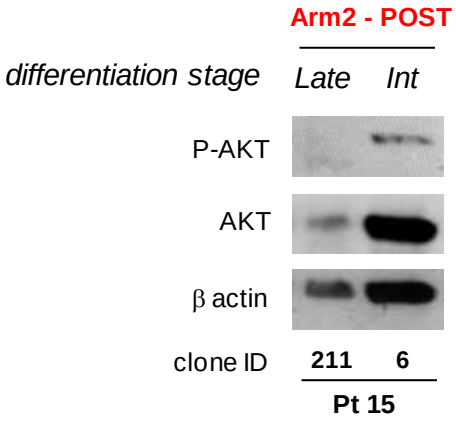

Int = Intermediate Differentiated (CD28$^-$CD27$^+$); Late = Late Differentiated (CD28$^-$CD27$^-$)

Figure S5. Expression of pSer473-AKT in gp100-specific T-cell clones. Western Blot analysis of AKT activation (pSer473 -AKT) and total AKT tested on whole cell extracts of 1.5 x10^6 viable cells of representative gp100-specific clones (n = 2) after treatment (POST) from Pt15 (Arm2), 18 h following activation by plate-coated anti-CD3 mAb. Gel loading control was performed analyzing total β-actin. The differetiation stage, based on the expression of CD28 and CD27 molecules (see Table1), for each clone is indicated.

Figure S6

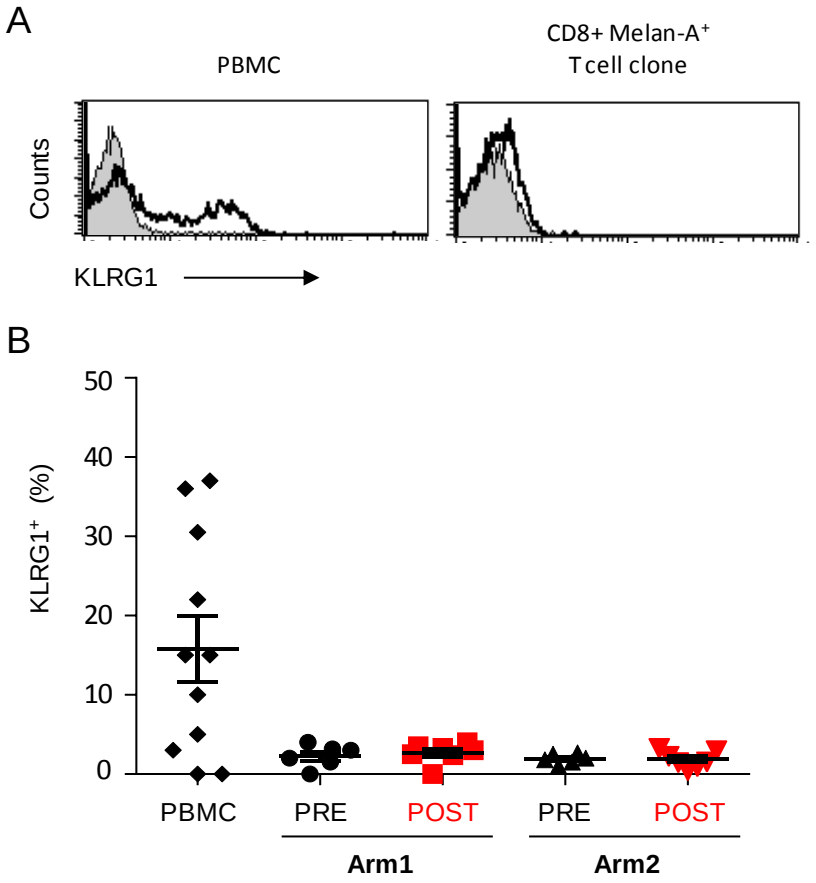

Figure S6. Melan-A-specific T-cell clones do not express KLRG1. (**A**) Representative flow cytometric analysis for the expression of KLRG1 receptor (open histograms) in total PBMC from healthy donor (left) and in a representative Melan-A-specific T-cell clone (right). Isotype control for KLRG1 mAb is shown as overlaid filled histogram. Staining was performed after 48h (not shown) and 72h stimulation with plate-bound anti-CD3 mAb (2 µg/ml). (**B**) Pooled data from control PBMCs and T-cell clones, where each dot represents the mean value from three independent experiments. Mean ± SEM is shown.